arXiv:1407.1653v1 [nucl-th] 7 Jul 2014

Final-state interactions in deep-inelastic scattering from a tensor polarized deuteron target.

Wim Cosyn

Department of Physics and Astronomy, Ghent University, Proeftuinstraat 86, 9000 Gent, Belgium

E-mail: wim.cosyn@ugent.be

Misak Sargsian

Department of Physics, Florida International University, Miami, Florida 33199, USA

Abstract. Deep-inelastic scattering (DIS) from a tensor polarized deuteron is sensitive to possible non-nucleonic components of the deuteron wave function. To accurately estimate the size of the nucleonic contribution, final-state interactions (FSIs) need to be accounted for in calculations. We outline a model that, based on the diffractive nature of the effective hadron–nucleon interaction, uses the generalized eikonal approximation to model the FSIs in the resonance region, taking into account the proton-neutron component of the deuteron. The calculation uses a factorized model with a basis of three resonances with mass $W < 2$ GeV as the relevant set of effective hadron states entering the final-state interaction amplitude for inclusive DIS. We present results for the tensor asymmetry observable A_{zz} for kinematics accessible in experiments at Jefferson Lab and Hermes. For inclusive DIS, sizeable effects are found when including FSIs for Bjorken $x > 0.2$, but the overall size of A_{zz} remains small. For tagged spectator DIS, FSIs effects are largest at spectator momenta around 300 MeV and for forward spectator angles.

1. Introduction

Deep-inelastic scattering (DIS) from a polarized spin 1 target yields access to new structure functions not present for the spin 1/2 case [1]. The leading twist structure function b_1 is accessible in DIS from a tensor polarized spin 1 target with an unpolarized beam. In the parton model, b_1 is sensitive only to the spin of the embedding spin 1 hadron. For a spin 1 system of two non-interacting spin 1/2 particles at rest, b_1 is trivially zero. For the deuteron, due to the D-wave admixture in the wave function of a few percent, b_1 is still expected to be small ($b_1 \ll F_1^D$) in the plane-wave approximation. At low Bjorken $x < 0.1$, shadowing effects are expected to yield significant contributions to b_1 [2, 3, 4]. Measurement of a sizeable value for b_1 at moderate x would provide insight into possible non-nucleonic components in the deuteron [5]. The Hermes collaboration measured b_1 for $0.01 < x < 0.45$ at $0.5 < Q^2 < 5$ GeV^2, finding non-zero values and the measured tensor asymmetry A_{zz} [see Eq. (8) below] exhibited a sign change around $x \approx 0.3$ [6]. An experiment at Jefferson Lab (JLab) will provide a new measurement for b_1 at $0.16 < x < 0.5$ and $1 < Q^2 < 5$ GeV^2 [7].

So far, no study has been made of possible final-state interaction (FSI) effects at moderate x to the nucleonic contribution of b_1. It is important to quantify this contribution as a sizeable FSI

effect could dominate possible non-nucleonic contributions. Here, we present work in a model that has been used to account for FSIs in DIS from the deuteron for inclusive [8] and tagged spectator measurements [9, 10]. The major difficulty in describing FSI in these reactions is that one lacks detailed information about the composition and space-time evolution of the hadronic system produced in the deep inelastic scattering and how this changes as a function of Bjorken x and Q^2.

2. Formalism

The model introduced in Ref. [9] accounted for FSI effects in DIS from the deuteron based on general properties of high-energy diffractive scattering. The underlying assumption was that due to the restricted phase space (finite values of W and Q^2), the minimal Fock state component of the wave function can be used to describe DIS from the bound nucleon. In this case the scattered state consists of three outgoing valence quarks whose rescattering from the spectator nucleon is parametrized in the form of a Q^2- and W-dependent diffractive amplitude.

The model uses the virtual nucleon approximation (VNA) [11, 12, 13] to describe DIS from the deuteron. In the VNA, only the proton-neutron component of the deuteron system is considered. It is also assumed that the negative energy projection of the virtual nucleon propagator gives negligible contributions to the scattering amplitude and the contribution of meson exchange currents is neglected. In the VNA, the nuclear wave function $\Psi_D(p)$ is normalized to account for baryon number conservation [14]:

$$\int \alpha |\Psi_D(p)|^2 d^3p = 1, \tag{1}$$

where $\alpha = 2 - \frac{2(E_s - p_{s,z})}{M_D}$ is the light cone momentum fraction of the deuteron carried by the bound nucleon, with $E_s(p_s)$ the on-shell energy (momentum) of the spectator nucleon. Because of the virtuality of the interacting nucleon it is impossible to satisfy the momentum sum rule at the same time, which can be qualitatively interpreted as part of the deuteron momentum fraction being distributed to non-nucleonic degrees of freedom.

The final-state interaction contribution is encoded in a Feynman diagram where after the interaction of the virtual photon with the bound nucleon, the produced hadronic mass X interacts with the spectator nucleon through an effective rescattering amplitude. At the energies for the experiments considered here, we can assume that the rescattering will be highly diffractive and will occur over small angles and the generalized eikonal approximation (GEA) [15] can be applied. In the GEA an eikonal form is adopted for the effective rescattering amplitude:

$$f_{X'N,XN} = \sigma(Q^2, x)(i + \epsilon(Q^2, x))e^{\frac{B(Q^2,x)}{2}t}, \tag{2}$$

where σ, ϵ and B are the effective total cross section, real part and the slope factor of the diffractive $X'N \to XN$ scattering amplitude. The x and Q^2 dependence of the scattering parameters σ and B were determined by fitting our model calculations to data for tagged spectator deuteron DIS taken in the Deeps experiment at Jefferson Lab [9, 16]. In the derivation of the FSI amplitude, a factorized approach is used, whereby the interaction of the virtual photon with the off-shell nucleon (encoded in the nucleon structure functions) is taken out of the integration over the intermediate spectator momentum. Finally, the four structure functions for tagged spectator deuteron DIS (F_T, F_L, F_{LT}, F_{TT}) can be written as the product of a distorted deuteron momentum distribution containing the amplitude of Eq. (2), the nucleon structure function F_2^N and kinematical factors (for detailed expressions see Ref. [9]).

By applying the optical theorem to the forward virtual Compton scattering amplitude, the model was extended to inclusive deuteron DIS in Ref. [8] :

$$W_D^{\mu\nu} = \frac{1}{2\pi M_D}\frac{1}{3}\sum_{s_D} \Im m\, \mathcal{A}^{\mu\nu}_{\gamma^* D}(t=0)\,, \tag{3}$$

where $W_D^{\mu\nu}$ is the hadronic tensor of the inclusive DIS process and $\mathcal{A}^{\mu\nu}_{\gamma^* D}$ the virtual Compton scattering amplitude. The advantage of such an approach is that the amplitudes accounting for the FSI effects will self-consistently satisfy the unitarity conditions for inelastic rescattering. The amplitude $\mathcal{A}^{\mu\nu}_{\gamma^* D}$ contains contributions from the plane-wave diagram and the rescattering diagram, where the produced hadronic mass X interacts with the spectator nucleon. Again, a factorized approximation is applied and for the intermediate hadronic states three effective resonances (at invariant mass $W = 1.232, 1.5$, and 1.75 GeV) were taken into account in addition to a broad contribution from the DIS continuum. We showed that in our formalism, FSI effects naturally disappear as Q^2 increases due to phase-space constraints and found sizeable FSI effects for $x > 0.6$ and $Q^2 < 10\text{GeV}^2$.

It is now straightforward to extend the model to the situation of a polarized deuteron target. It suffices to replace the average over the deuteron polarization by a trace with the appropriate spin 1 density matrix. Consequently, Eq. (3) can be written as

$$W_D^{\mu\nu} = \frac{1}{2\pi M_D}\sum_{\lambda\lambda'} \Im m\, \rho^D_{\lambda'\lambda}\left[\mathcal{A}^{\mu\nu}_{\gamma^* D}(t=0)\right]_{\lambda\lambda'}\,, \tag{4}$$

where ρ^D represents the spin 1 density matrix for the deuteron.

3. Deuteron density matrix

The density matrix for a spin 1 particle in a rest frame for the particle can be written in a multipole expansion [17]

$$\rho^D_{\lambda\lambda'} = \frac{1}{3}\sum_{L=0}^{2}\sum_{M=-L}^{L}(2L+1)t^*_{LM}\left(\hat{T}^L_M\right)_{\lambda\lambda'}\,, \tag{5}$$

where λ denotes the spin projection of the deuteron, t_{LM} are the multipole parameters, and the spherical tensor operators read $\left(\hat{T}^L_M\right)_{\lambda\lambda'} = \langle s\lambda | s\lambda'; LM\rangle$. When the ensemble is made up of particles quantized along the z-axis, the density matrix takes on a simple form

$$\rho^D = \frac{1}{3}\text{diag}(1+\frac{3}{2}P_z+2P_{zz}, 1-P_{zz}, 1-\frac{3}{2}P_z+2P_{zz})\,, \tag{6}$$

where $P_z = \sqrt{2}t_{10} = p^+ - p^-$ and $P_{zz} = \sqrt{10}t_{20} = p^+ + p^- - 2p^0$, with p^λ the probability of finding the deuteron with a spin projection λ along the x-axis.

In theoretical calculations for deuteron DIS, the hadronic tensor is usually evaluated in the hadron plane (determined by the virtual photon and spectator nucleon), with the z-axis along the virtual photon momentum. For a fixed target experiment, however, the deuteron density matrix is usually determined in a deuteron rest frame with the z-axis along the incoming beam. Consequently, care has to be taken to transform the density matrix to the hadron plane in order to do meaningful comparisons with experimental data. This involves a rotation over the angle between the incoming beam and virtual photon θ_{eq}, and over the angle ϕ between the electron and hadron planes. Due to the simple transformation properties under rotations of the multipole parameters in Eq. (5), this transformation can be readily computed [17]. For an ensemble with

only the multipole parameter t_{20} nonzero in the rest frame with the z-axis along the incoming beam, one obtains for the multipole parameters $\hat{t}_{LM}$ in the hadron plane [18]:

$$\hat{t}_{20} = \frac{1}{4}(1 + 3\cos 2\theta_{eq})\, t_{20}\,,$$
$$\hat{t}_{21} = -\sqrt{\frac{3}{8}}\sin 2\theta_{eq} e^{i\phi}\, t_{20}\,,$$
$$\hat{t}_{22} = \sqrt{\frac{3}{32}}(1 - \cos 2\theta_{eq}) e^{i2\phi}\, t_{20}\,. \tag{7}$$

For the deuteron DIS formalism under consideration here, this means that even after integrating over the angle ϕ (which is done in the inclusive DIS formalism), the cross section will receive contributions from the F_{LT} and F_{TT} response functions (that come with a $\cos\phi$ and $\cos 2\phi$ dependence) through respectively the $\hat{t}_{21}$ and $\hat{t}_{22}$ parts of the density matrix.

4. Results

The cross section for DIS from a polarized deuteron target without any beam polarization can be written as

$$d\sigma = d\sigma_u(1 + \frac{1}{2}P_{zz}A_{zz})\,, \tag{8}$$

where σ_u is the cross section for an unpolarized target, P_{zz} was defined in Eq. (6), and A_{zz} is the tensor asymmetry of the deuteron cross section which can be related to the structure function b_1 [6]. For the calculations of A_{zz} for inclusive DIS from the deuteron, we include resonances at invariant mass $W = 1.232, 1.5$, and 1.75 GeV as the set of effective hadron states entering the final-state interaction amplitude. The values of the scattering parameters in Eq. (2) are taken from our fits to the JLab Deeps data. We used the SLAC nucleon structure function parametrization [19] and for the non-relativistic deuteron wave function, we use the parametrization based on the Paris NN potential [20].

In Fig. 1, we present calculations of A_{zz} for inclusive DIS from the deuteron for kinematics accessible in the upcoming JLab experiment [7]. For the plane-wave calculations, we observe that A_{zz} is almost zero for Bjorken x in the DIS region, while it reaches values of the order of $\sim \pm 0.01$ in the resonance region at $Q^2 = 2$ GeV^2 and becomes smaller with increasing Q^2. Adding the FSI contributions has a significant effect on the size of A_{zz} over the whole x range. At $Q^2 = 2$ GeV^2 the off-shell contribution of the FSI diagram also has a sizeable contribution while at $Q^2 = 5$ GeV^2 it is almost negligible. It is worth remarking that even though the effective hadronic states taken into account in the FSI diagram all lie in the resonance region, they also contribute significantly to A_{zz} in the DIS region. This can be understood in the following manner. In the formalism A_{zz} is only nonzero because of the D-wave component of the deuteron wave function, both in the plane-wave and FSI contribution to the cross section. As the dominant contribution for the D-wave occurs at momenta above 250 MeV, A_{zz} is still sensitive to the resonance region FSI contributions in the DIS x-region for free nucleon kinematics due to the Fermi motion of the struck nucleon. Comparing the effect of tensor polarization along the virtual photon with polarization along the incoming beam, we find limited differences for $Q^2 = 5$ GeV^2. For $Q^2 = 2$ GeV^2 the size of A_{zz} decreases, especially at the largest x values, where the angle θ_{eq} is largest.

In Fig. 2, we show similar A_{zz} calculations as in Fig. 1 but for kinematics covered in the Hermes experiment [6]. Similar observations as in Fig. 1 apply. The difference between the left and right panel for $Q^2 = 1$ GeV^2 is more pronounced here because of larger θ_{eq} values, with A_{zz} values including FSIs becoming significantly smaller for the case of polarization along the incoming beam. Comparing our calculation to the Hermes data point of $A_{zz} = 0.157 \pm 0.69$ at $x = 0.45$, $Q^2 \approx 5$GeV^2, we find a value of $A_{zz} \approx 0.0015$, about two orders of magnitude smaller.

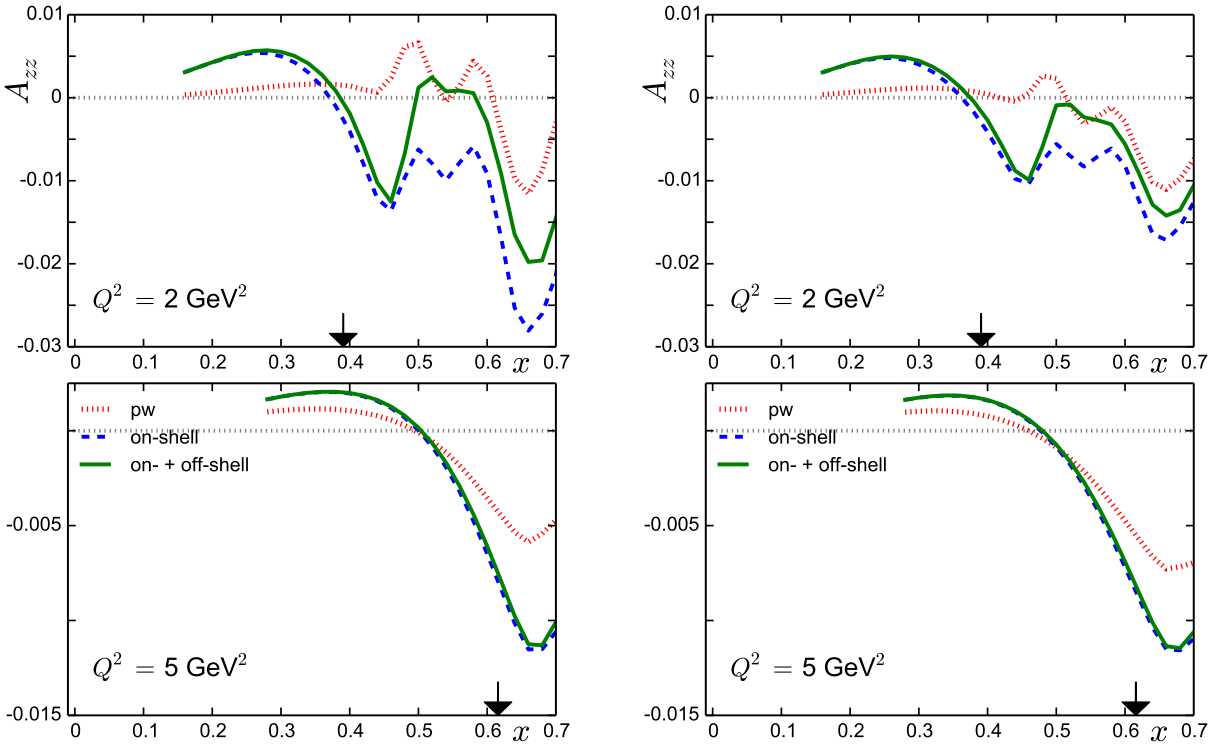

Figure 1. Tensor asymmetry A_{zz} for kinematics accessible in the upcoming JLab experiment [7] (incoming beam of 11 GeV). The red dotted curve shows the plane-wave calculations, the blue dashed (green full) curve includes the contribution of the on-shell (and off-shell) FSI contribution. For details on the FSI on- and off-shell calculations, we refer to Ref. [8]. Left panels have the deuteron polarized along the virtual photon direction, right panels along the incoming beam, with the transformation according to Eq. (7). The arrow along the x-axis indicates the boundary at $W = 2$ GeV between the resonance and DIS regions for free nucleon kinematics.

Finally, in Fig. 3, we show calculations for tagged spectator DIS $[D(e, e'p_s)X]$ from the deuteron at different spectator momenta and two values of the invariant mass W of the produced X, for a deuteron polarized along the virtual photon momentum. One observes that the plane-wave calculations produce sizeable values for A_{zz} in the case of intermediate spectator momenta of 340 MeV (where the deuteron D-wave contribution is largest), especially for forward spectator angles. Including FSIs has little effect at the low spectator momentum of 100 MeV, but causes significant changes for higher spectator momenta in the forward region, where we know from our previous study [9] that FSI effects are largest in the unpolarized cross section. For $p_s = 340$ MeV and $\cos\theta_s > 0.5$ including the FSI contribution even reverses the sign of A_{zz}.

5. Conclusion

We presented calculations for the deuteron tensor asymmetry A_{zz} in a model based on the virtual nucleon and generalized eikonal approximations that allows for the description of final-state interaction effects for deuteron DIS reactions from intermediate hadronic states in the resonance region. For inclusive DIS, we included resonances at invariant mass $W = 1.232, 1.5$, and 1.75 GeV as the set of effective hadron states entering the final-state interaction amplitude. Our calculations for kinematics accessible at JLab12 and Hermes showed sizeable FSI effects both in the resonance and DIS region for free-nucleon kinematics, though the overall size of

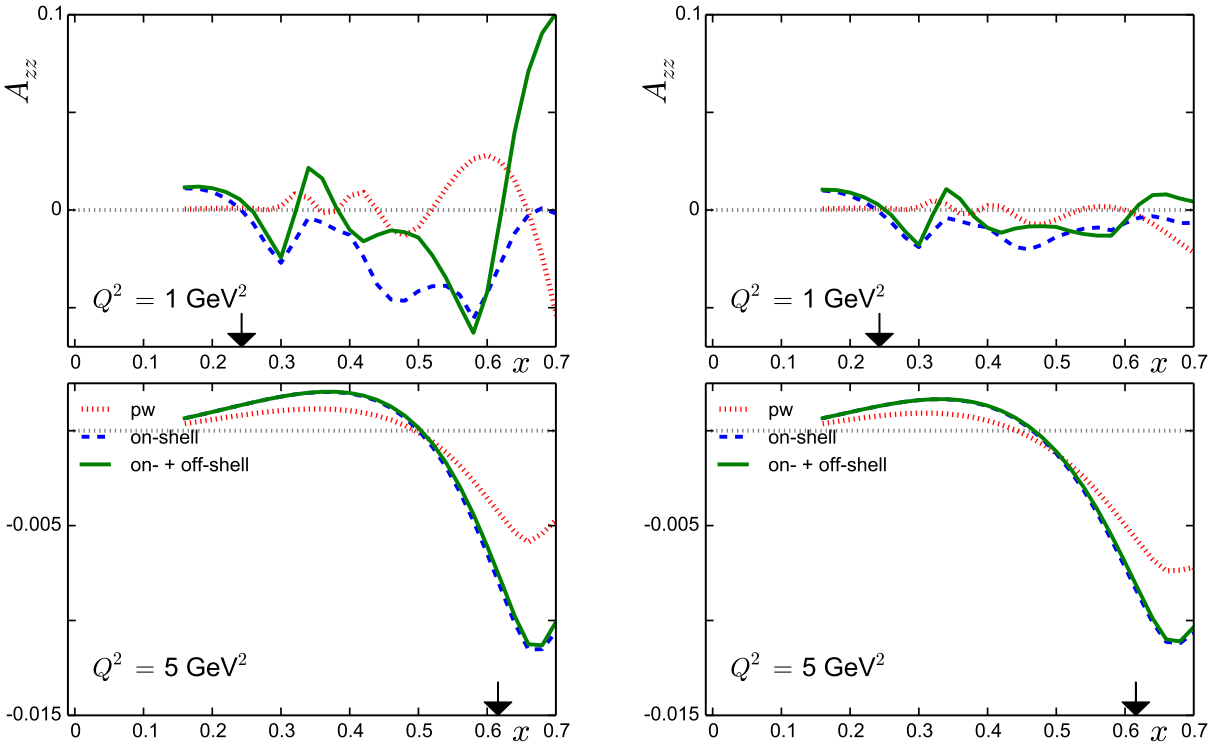

Figure 2. Tensor asymmetry A_{zz} for kinematics covered in the Hermes experiment [6] (incoming beam of 27.6 GeV). Curves and panels as in Fig. 2

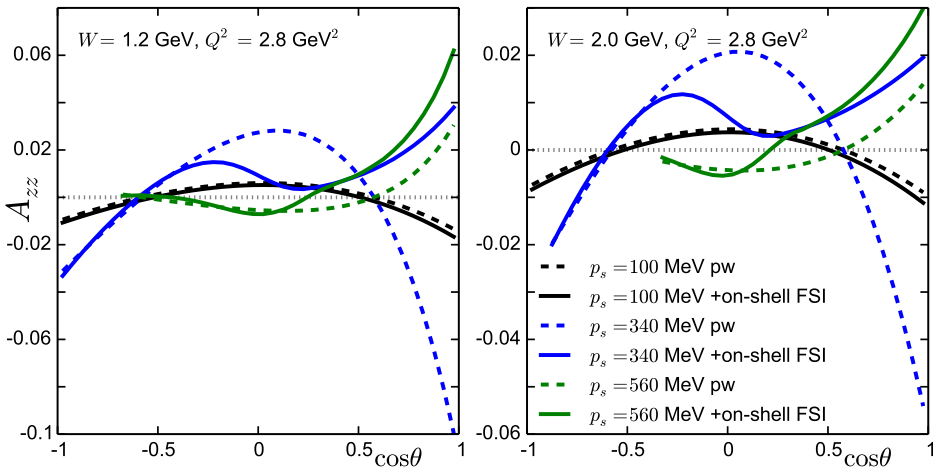
$W = 1.2$ GeV, $Q^2 = 2.8$ GeV^2
$W = 2.0$ GeV, $Q^2 = 2.8$ GeV^2
A_{zz}
cosθ
p_s =100 MeV pw
p_s =100 MeV +on-shell FSI
p_s =340 MeV pw
p_s =340 MeV +on-shell FSI
p_s =560 MeV pw
p_s =560 MeV +on-shell FSI

Figure 3. Tensor asymmetry for tagged spectator DIS $D(e, e'p_s)X$ at invariant mass W of X 1.2 (left panel) and 2.0 GeV (right panel) for three different spectator momenta. Full (dashed) curves represent a plane-wave (including FSIs) calculation. For details on the FSI calculations, see Ref. [9].

the nucleonic contribution to A_{zz} remains small. The sensitivity of A_{zz} in the DIS region to FSI contributions from the resonance region can be understood from the dependence of the

A_{zz} observable on the D-wave part of the deuteron wave function. We showed that deuteron polarization along the incoming beam reduces the size of A_{zz} at the low Q^2 values compared to polarization along the virtual photon direction. For the tagged spectator DIS process FSI effects proved to be largest at spectator momenta around 300 MeV and for spectator angles $\cos\theta_s > 0.5$.

Acknowledgments
The computational resources (Stevin Supercomputer Infrastructure) and services used in this work were provided by Ghent University, the Hercules Foundation and the Flemish Government department EWI. This work is supported by the Research Foundation Flanders as well as by the U.S. Department of Energy Grant under Contract DE-FG02-01ER41172.

References

[1] Hoodbhoy P, Jaffe R and Manohar A 1989 *Nucl.Phys.* **B312** 571
[2] Nikolaev N N and Schafer W 1997 *Phys.Lett.* **B398** 245–251 (*Preprint* hep-ph/9611460)
[3] Edelmann J, Piller G and Weise W 1997 *Z.Phys.* **A357** 129–131 (*Preprint* nucl-th/9701026)
[4] Bora K and Jaffe R 1998 *Phys.Rev.* **D57** 6906–6911 (*Preprint* hep-ph/9711323)
[5] Miller G A 2014 *Phys.Rev.* **C89** 045203 (*Preprint* 1311.4561)
[6] Airapetian A *et al.* (HERMES Collaboration) 2005 *Phys.Rev.Lett.* **95** 242001 (*Preprint* hep-ex/0506018)
[7] Slifer K and Long E 2014 *PoS* **PSTP2013** 008 (*Preprint* 1311.4835)
[8] Cosyn W, Melnitchouk W and Sargsian M 2014 *Phys.Rev.* **C89** 014612 (*Preprint* 1311.3550)
[9] Cosyn W and Sargsian M 2011 *Phys. Rev.* **C84** 014601 (*Preprint* 1012.0293)
[10] Cosyn W and Sargsian M 2011 *AIP Conf.Proc.* **1369** 121–128 (*Preprint* 1101.1258)
[11] Melnitchouk W, Sargsian M and Strikman M I 1997 *Z. Phys.* **A359** 99–109 (*Preprint* nucl-th/9609048)
[12] Sargsian M and Strikman M 2006 *Phys. Lett.* **B639** 223–231 (*Preprint* hep-ph/0511054)
[13] Sargsian M M, Simula S and Strikman M I 2002 *Phys. Rev.* **C66** 024001 (*Preprint* nucl-th/0105052)
[14] Frankfurt L L and Strikman M I 1981 *Phys. Rept.* **76** 215–347
[15] Sargsian M M 2001 *Int. J. Mod. Phys.* **E10** 405–458 (*Preprint* nucl-th/0110053)
[16] Klimenko A V *et al.* (CLAS) 2006 *Phys. Rev.* **C73** 035212 (*Preprint* nucl-ex/0510032)
[17] Leader E 2005 *Spin in Particle Physics (Cambridge Monographs on Particle Physics, Nuclear Physics and Cosmology)* (Cambridge University Press) ISBN 0521020778
[18] Jeschonnek S and Van Orden J W 2009 *Phys.Rev.* **C80** 054001 (*Preprint* 0907.3712)
[19] Bodek A, Breidenbach M, Dubin D L, Elias J E, Friedman J I, Kendall H W, Poucher J S, Riordan E M, Sogard M R, Coward D H and Sherden D J 1979 *Phys. Rev. D* **20** 1471–1552
[20] Lacombe M *et al.* 1980 *Phys. Rev.* **C21** 861–873